Heliyon

Desorption of harmful hydrocarbon compounds in soil using micron-sized magnetic particles and high-frequency magnetic fields

Bailey S. Tye, Rushi J. Vyas *

Department of Electrical Engineering, University of Calgary, Calgary, AB T2N1N4, Canada

* Corresponding author.

E-mail address: rushi.vyas@ucalgary.ca (R.J. Vyas).

Abstract

This research looks at the use of high frequency (HF) magnetic fields to desorb/ reduce harmful chemical compounds within gasoline and diesel that commonly leak out of underground storage tanks. Using a multi-strand coil design, measured magnetic fields of over 3 kilo-amperes per meter are generated at an optimal frequency of 117 kHz without skin-depth losses, and without the use of expensive super-conductors or liquid-cooled mechanisms. This high frequency magnetic field is successfully used in non-contact-based magnetic heating and desorption of Gasoline and Diesel mixed with sand, water and easily-dispersible, benign micrometer-sized iron filings, used as a magnetic absorber. Gas chromatography (GC) tests done on magnetically-heated Gasoline-soil and Diesel-soil mixtures show desorption/reduction of gasoline and diesel by 44% and 51% respectively, but desorption/reduction of harmful BTEX compounds and other chemical irritants within Gasoline and Diesel by 28–66% after only 80 minutes of magnetic heating. Review of remediation/desorption methods show magnetic fields fare favorably in comparison to other methods that require longer treatment period or the use of secondary pollutants at reducing hydrocarbon and BTEX compounds in them.

1. Introduction

Environmental consultants estimate that 90% of gas stations built prior to 1970 are contaminated due to underground storage tanks (UST) leaking hydrocarbons into soil and water [1]. While UST leak statistics in Canada are hard to come by, in the US alone over 5,32,000 UST leaks have occurred as of September 2016 [2]. In addition to UST, oil and gas pipelines are another major source of hydrocarbon contamination of soil and water, with 6.4 million liters of hydrocarbons having leaked in the Canadian province of Alberta alone [3]. Major contaminants of concern are petroleum hydrocarbons (PHC); BTEX compounds namely Benzene, Toluene, Ethylbenzene and Xylene and Polycyclic aromatic hydrocarbons (PAH) that are added or present in Hydrocarbons during the refining process [4]. Ex-situ methods to remediate hydrocarbon-contaminated soil involve excavating and transporting soil to distant landfills. Depending on hauled weightage and distance, ex-situ treatment costs can vary from 100,000 to several million Canadian dollars. In mid-sized cities and rural areas, older gas stations often are shut-down and left in a contaminated state due to land resale and property taxes being much lower than ex-situ remediation costs [1].

The purpose of this study is to examine whether magnetic heating, with the addition of magnetic enhancers, is an effective means of removing hydrocarbon materials from contaminated soil. We then compare this to current technologies and discuss the advantages and disadvantages associated with our method.

2. Background

In-situ remediation methods involve chemical or electrical heat treatments to neutralize or desorb hydrocarbon contaminants. Chemical treatments of soil can reduce hydrocarbon contaminants with a removal efficiency of 27–97% [5]. Thus, excess chemical oxidizers to ensure a more complete reduction of contaminants are a common practice, which leads to secondary chemical pollution. Chemical oxidizers using Permanganates or Peroxides (Fenton) solidify or evaporate at cold or hot temperatures respectively, which limits their dispersion through the soil sub-surface and hence their effectiveness at reducing hydrocarbon contaminants in soil [6], [7]. By comparison electrically heating contaminated soil has been shown to desorb contaminants with removal efficiencies higher than 90% without causing secondary pollution albeit with higher input energy [8]. However, Electrical resistive heating (ERH) requires 50–80 kilowatts of input power and close contact between buried electrodes and the contaminants for weeks for effective contaminant treatment [9]. Newer, cleaner, and more efficient techniques to treat

soil and water contaminated with hydrocarbons without adding additional chemical pollutants are necessary for North America's environment and hydrocarbon-heavy economy.

In comparison to contact-based ERH, contact-less magnetic fields can penetrate through most non-magnetic materials, which include soil, water, and other organic matter within a certain distance from a magnetic coil. While hydrocarbons as a whole are considered non-magnetic or diamagnetic, some harmful compounds within hydrocarbons such as Benzene have been shown to internally generate an aromatic ring current in response to an incident magnetic field, which may aid in a compound's desorption [10].

The purpose of this research is two-fold: Firstly, this work develops a low-cost and energy-efficient magnetic-heating setup that produces kilo-amperes per meter of magnetic field intensities at high frequency bands to induce over 80 degrees Celsius rise in hydrocarbon-soil-water mixtures. This setup works without external water-cooling mechanisms, and uses low-cost materials, which are easily adaptable to in-situ ground environment. Secondly this work offers a detailed and measured analysis of the effects of higher magnetic field intensities at HF bands in the desorption of specific harmful hydrocarbon compounds found in Gasoline and Diesel such as Benzene, Toluene, Ethylbenzene, Xylene and other irritants. We also show the method of achieving high kA/m magnetic field intensities by using resonant Litz coils that have to be wound to provide the right impedance for a high-frequency current amplifier. The Alberta guidelines require 0.68 mg/L of hydrocarbons for fine, and 0.40 mg/L for coarse soils with different limits for specific compounds within Gasoline and Diesel [11]. In this paper, a magnetic field with a frequency of 117 kHz, produced by a multi-strand coil, is used to reduce hydrocarbon concentrations to within guideline limits.

Current research involving magnetic heating is presented in [12, 13, 14]. Their applications however are different. They focus on using magnetic fields to heat small concentrations of specially fabricated ferro-magnetic nano-compounds to treat hypothermia in biomedical applications. In [12] and [14] magnetic field intensities of kA/m, at between 233 and 370 kHz, are used to heat $MgFe_2O_4$ powder-bead-milled to nano-sized. In these prior works, technical information, and measured verification of obtaining kA/m scale magnetic field intensities at these frequency bands are not presented. Also, a temperature-rise of only 35 degrees Celsius above room temperature in 20 minutes using specially milled and expensive $MgFe_2O_4$ nanoparticles may prove insufficient and uneconomical for desorbing hydrocarbons from larger tracts of soil. To be able to desorb hydrocarbons from large amounts of soil, the concentration of magnetic particles to non-magnetic soil/water will have to be very low to satisfy economic feasibility. Also, the coil used in [14] needs an externally-pumped water-cooling mechanism,

which would require costly water haulage, and would also prove impractical for in-situ heating of soil and water to remove hydrocarbons.

3. Design

The magnetic field (B) induced in a material with magnetic permeability of μ, placed in the middle of a coil of radius R, with N turns, and carrying current I is given by the simplified expression in (1) [15].

$$\overline{B} = (\mu' + j\mu'')\overline{H} = (\mu' + j\mu'')\frac{IN}{2R} \tag{1}$$

Heat induced in a material due to a magnetic field can be increased by increasing the imaginary permeability of the material (μ"), or by increasing the intensity of the magnetic field itself. While the complex permeability of sand and water are close to 0 due to their diamagnetic nature, the addition of low-cost, non-toxic iron filings, with a peak imaginary permeability of 50, dispersed into the soil or water mixture can increase the overall heat-transducing ability. The iron filings act as a magnetic enhancer to aid the desorption process [16], [17]. Table 1 shows the imaginary permeability of the compounds used. The complex magnetic permeability of most materials varies with frequency with iron powder peaking when exposed to magnetic fields close to 100 kHz [17].

In addition to using this optimal frequency, the magnetic field intensity through a fixed area is also increased by the number of turns of wire in the coil and the current through each of those turns. A plot of the maximum current carrying capacity and the frequency cutoff for 100% skin depth for different diameters of wire is shown in Fig. 1, and shows a trade-off between the maximum current carrying capacity of a wire and the frequency of the current. To allow for 100% skin depth at 100 kHz, we used multi-strand wire (litz wire) consisting of 435 strands. This number of strands was chosen based on commercial availability of high strand litz wire, and the lengths available.

Table 1. Magnetic Complex Permeability of materials used. Relative to the permeability of a vacuum being 1. [16, 17, 18].

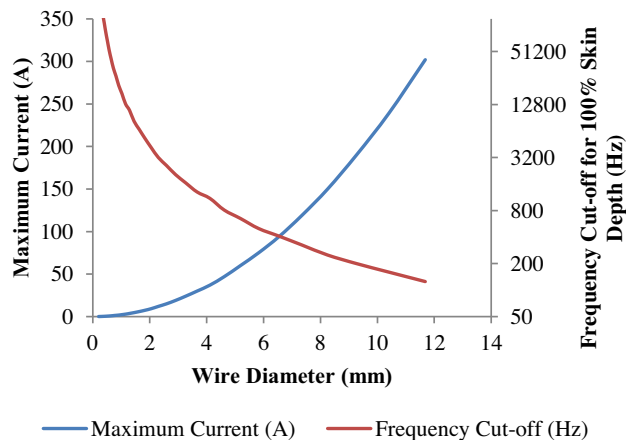| Material	Imaginary Permeability (μ_r)
Gasoline	unknown
Diesel	unknown
Sand	0-0.25 @ 100 kHz − 10 MHz
Water	0
Iron	50 @ 100 kHz
Iron oxide	0-0.5 @ 100 kHz; 3 @ 1 GHz

Fig. 1. Maximum current rating and frequency cut-off versus wire diameter.

It is important to note that for maximum current output, current amplifiers like to see a certain output impedance, and a coil has to be designed to provide this optimum impedance at the specified frequency. In our case we used an Accel TS-250 current amplifier which provided information of the amplifier's current gain over its operating bandwidth. We designed a resonant Litz coil that provided a near-optimal impedance for the current amplifier to output its near maximum amplitude of 3 A at near 100 kHz. The resonance frequency will change rapidly based on the inductance, and capacitance of a coil. Therefore, calculations must be done when redesigning or slightly altering the design of the coil, and maybe even with drastic ambient temperature changes.

The final coil was designed with an inner radius of 1.5 cm, height of 10 cm, and wrapped to form approximately 135 turns. The impedance of the multi-strand coil was measured using a Hewlett Packard 4194A impedance analyzer, and is shown in Fig. 2. The coil showed a low AC resistance between 0.58 ohms and 1.85 ohms from frequencies 80 kHz to 150 kHz, where the enhancers show the highest complex permeability. The current amplifier is expected to give out near peak current amplitude of 3A in this frequency range. The coil also showed a reactance of between 144 and 259 ohms in the same frequency band. To ensure resonance by the coil and maximize current output, it was calculated that a 6.6 nF series capacitor would cancel out the 200.16 µH inductance of the coil [19]. However, in the final coil design a 6 nF power capacitor capable of handling 6 amps with a self-resonant frequency of over 100 kHz had to be used due to part availability. As a result, the resonance of the tuned coil was shifted slightly to a higher frequency of 117–118 kHz as shown by the coil's reactance of 0 at that frequency in Fig. 2 (left).

Although a magnetic core may have boosted the field from our coil we did not use one. This was for two reasons: the samples needed to be placed at the center for highest field absorption, and the samples themselves, with added iron filings, acted
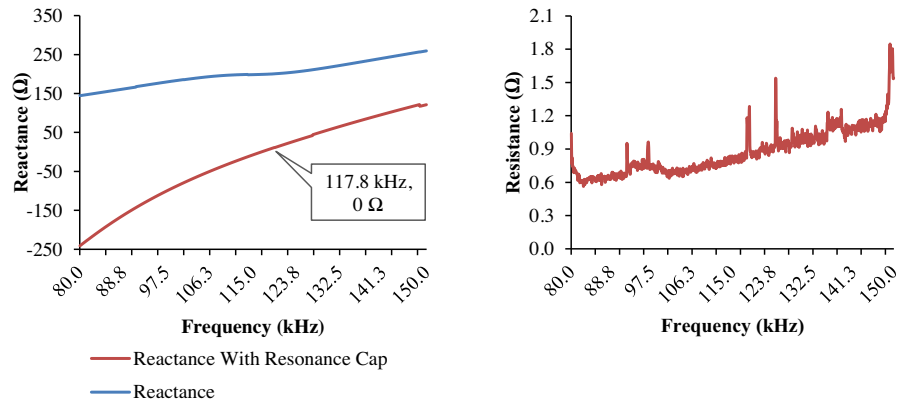
Fig. 2. (Left) Reactance of coil. The resonance shifted slightly in testing to 117.8 kHz due to heat, and small shifts of parts during transportation. (Right) Resistance of coil. The value of 0.87 Ω at 117.8 kHz allowed the current amp to easily supply full current. The random peaks are seen due to movements/ bends of the cable setup during measurements.

as a weak core. This effect was negligible for the final tests however, due to the iron concentration being so low.

Using Ampere's law, the magnetic field intensity (H) in the middle of the coil, with a coil length (h) of 10 cm and 135 turns (N), each carrying a near maximum current amplitude of 2.75 A (I), can be estimated using (2). In the middle of the coil where the soil-water-hydrocarbon test sample is placed, the field intensity is estimated to be 3712.5 A/m. This was the best field we could achieve with the current amplifier and Litz wire length and types available to us. Custom manufactured Litz wire, with a custom current amplifier, can be used to produce a higher magnetic field intensity, and flux density, heating the hydrocarbon-sand-iron particle mix at a quicker rate.

$$H = \frac{NI}{h} \qquad (2)$$

4. Experimental

The final setup used in the desorption tests is shown in Fig. 3 below. The function generator provides a low power signal to the current amplifier where it is amplified to a near maximum amplitude of 2.75 A. The coil reached a maximum of 49 °C after the longest test of 80 minutes. This shows the effectiveness of the multi-strand wire, keeping the coil at a cool temperature without the need for external cooling mechanism, which is important to maintain a stable supply current.

A stable magnetic field was induced at close to the resonant frequency of 117 kHz through the hydrocarbon-soil-water mix placed within the coil. Due to size constraint, the magnetic field intensity produced by the coil was measured just
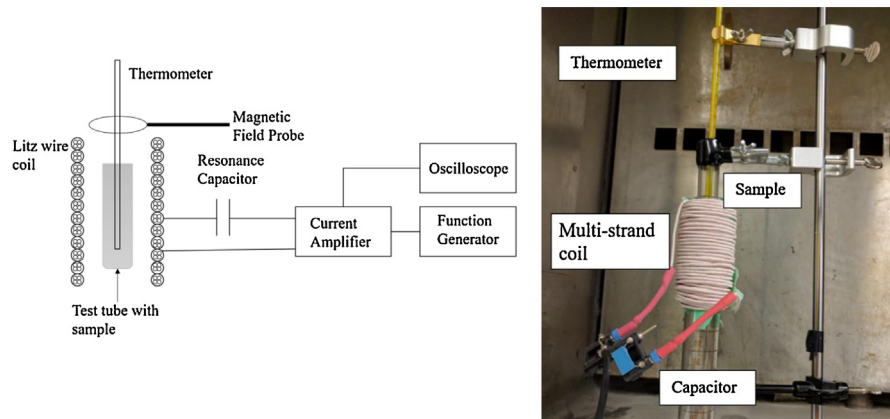
Fig. 3. (Left) Setup diagram, (Right) Setup photograph. The thermometer used was alcohol based, to not interfere with field. The clamp, and metal support were tested to verify they do not interfere with field generation. The support rod is not magnetic.

above the coil using an Aaronia magnetic near-field probe along with a Spectran NF5035 spectrometer. Sweeping the frequency of the field near the resonant frequency band showed that the coil produced a magnetic field intensity of 3.13 kA/m at 117.8 kHz as shown by the field-intensity measurement in Fig. 4. The main reason this value is lower than the expected value from Eq. (2) is due to the measurement location. The theoretical result is calculated assuming a central position of the solenoid/coil, and assumes infinite length. Our probe was placed at the top of the coil, resulting in a lower field measurement.

While complex magnetic permeability of gasoline and diesel are unknown, the overall complex permeability of these hydrocarbons mixed with sand (μ_r" = 0 to 0.25) and water (μ_r" = 0) [16] was determined to be low; a 3.13 kA/m magnetic field intensity through the mixtures did not yield temperatures high enough for desorption of the hydrocarbons. To absorb the magnetic field, the samples were mixed with varying concentrations of fine iron oxide and iron particles. Both iron and iron oxide are widely available at extremely low costs, and not known to be
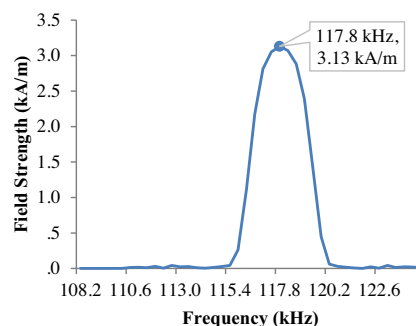

Fig. 4. Magnetic field measurement from the probes, showing a resonance at 117.8 kHz.

toxic to soil or water as per Alberta Tier 1 Soil and Groundwater Remediation Guidelines [11]. Tests with the addition of iron oxide did not yield high enough temperatures, which was due to iron oxide's low complex permeability at around 100 kHz (μ_r" = 0 to 0. 5) [18]. Iron particles on the other hand have a peak complex permittivity of 50 at around 100 kHz [17]. Furthermore, iron filings are readily available at particle sizes of around 1 μm, and can be readily mixed with water, soil, or in our case, sand particles with average sizes of 1 mm as shown in Fig. 5.

5. Results

Desorption rates of hydrocarbons depend on several material factors such as the relative grade, and weight which is decided by the crude variety and refining process. But in general, for all hydrocarbons desorption rates are higher at higher temperatures [20] [21].

5.1. Magnetic heating test results

Preliminary tests were run to measure just the conversion of magnetic field into heat by the sub-micron iron particles in sand. Five different sample mixtures with varying amounts of iron by weight were prepared, and placed within the coil, setup to generate 3.13 kA/m at 117.8 kHz. The temperature measurements were carried out using a non-metallic alcohol-based thermometer unaffected by the strong magnetic field. In real-world in-situ heating applications with magnetic fields, any magnetic enhancer like iron powder would have to be dispersed into the ground using water or something similar. Hence, some samples contained water to emulate the dispersing agent. The Sample mixtures prepared are shown in Table 2, and their magnetic heating results in Fig. 6. The tests were halted when the temperatures
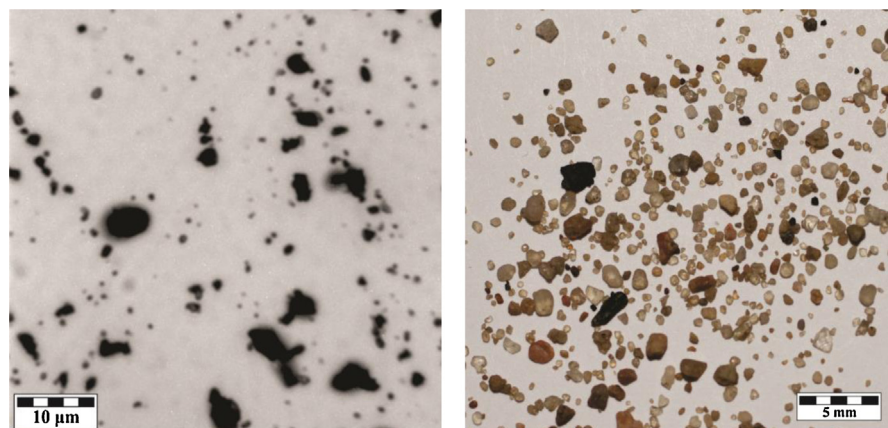

Fig. 5. (Left) Iron filings and clumps under a 40x microscope, (Right) Sand particles under a microscope.

Table 2. Sample contents for preliminary tests.

Sample	Heating Time (Minutes)	Contents	Percent Iron by weight	Maximum Temperature (°C)
1	8	5 mL water, 2.5 g iron	33	95
2	12	10 mL water, 1.25 g iron	20	93
3	45	15 g sand, 10 mL water, 1.25 g iron	5	78
4	30	5.6 g sand, 2.8 mL water, 1.4 g iron	14	92
5	25	15 g sand, 1.25 g iron	8	150

began to plateau, or in the case of sample 5, the temperature was too high for our measurement tools.

All five samples could successfully be magnetically heated over the initial evaporation point of gasoline (37–200 °C). While water was found to be an effective dispersing agent of sub-micron iron particles, magnetic heating in the presence of moisture slowed down the heating process as seen in samples 3, 4 and 5. Magnetic heating was found to be most effective when applied after enough time was given to allow the water to properly disperse iron particles through sand and evaporate substantially, as seen in the case of sample 5. Sample 5 contained only 8% iron by weight but was removed of moisture reaching temperatures of over 150 °C in just 25 minutes.

Magnetic heating of only water and iron particles showed the fastest rise in temperature due to the high percentage of iron, with samples 1 and 2 reaching boiling point in less than 5 minutes as shown in Fig. 6. Temperatures attained using magnetic heating were found to be high enough to desorb gasoline as its boiling
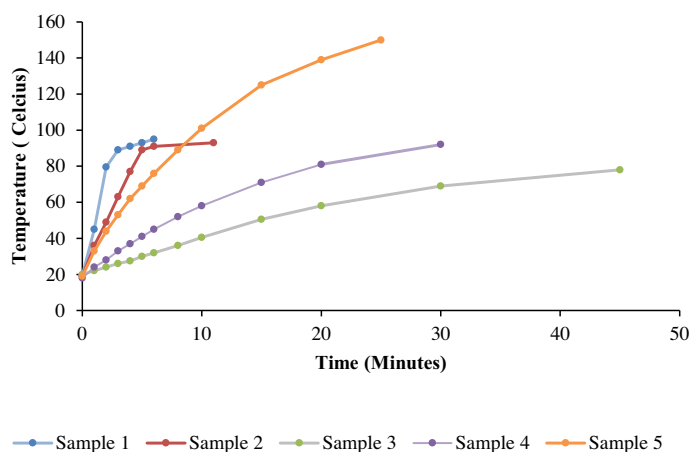

Fig. 6. Preliminary tests of different concentrations of iron, water, and sand as well as different mixing techniques. This is to simulate a way of distributing the iron into the ground in a full-scale application.

point ranges from 37–200 °C for different contained compounds [20]. Diesel has a much higher boiling point of 282–338 °C, but the amount of heat generated was found to be enough to desorb a portion of it [21] as shown by Gas Chromatography tests in the next section.

5.2. Sample preparation and specific absorption rate (SAR) nnalysis

The effect of magnetic heating on desorption of diesel, gasoline and specific compounds within each of the two, was determined using Gas Chromatography using a Hewlett Packard 5890 gas chromatograph (GC). Due to the difficulty of separating water impurities from the liquid chloroform agent used to dissolve hydrocarbon residues for GC tests, only dry samples of sand, micron-sized iron particles and hydrocarbons were used. Four identical samples were created each for Gasoline and diesel, and are shown in Table 3. Each sample was magnetically-heated for a different length of time and then dissolved in chloroform to extract the hydrocarbon residue from the soil-iron mix. All magnetic heating was carried out with a field intensity of 3.13 kA/m at 117.8 kHz. The magnetic heating profile of the samples measured is shown in Fig. 7.

To quantify the heating ability of the iron powder as a magnetic enhancer, the specific absorption rate (SAR) of the fuel-sand-iron mix was calculated using Eqs. (3) and (4) [22]. The specific heat complex was approximated based on the concentrations of components in the mixtures, and β was taken from the initial slopes of samples C, G in Fig. 7. The SAR of the gasoline-sand-iron and diesel-sand-iron mixes is determined to be 28.57 W/g, and 28.37 W/g respectively.

$$\beta = \frac{dT}{dt}\Big|t \to 0 = \frac{P}{C} \tag{3}$$

Table 3. Sample contents for GC analysis.

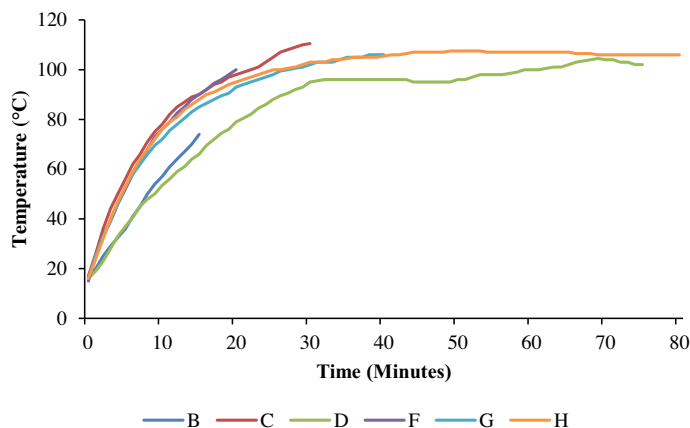| Sample	Heating Time (Minutes)	Contents (9% iron by weight)
A	0	1.25 mL gas (1.1 g), 36 g sand, 3.7 g iron filings
B	15	
C	30	
D	75	
E	0	1.25 mL diesel (1.1 g), 36 g sand, 3.7 g iron filings
F	20	
G	40	
H	80	

Fig. 7. Temperature vs heating time of samples B-H used for GC analysis. The variations in temperature rise rate can be attributed to uneven temperature pockets due to uneven iron particle distribution around the thermometer within samples B-H.

$$SAR_{Initial-slope} = \frac{P}{m_{MNP}} = \frac{\beta C}{m_{MNP}} \qquad (4)$$

β: Slope of the initial heat rise

T: Temperature of the mixture

t: Time

P: Power

C: Specific heat complex of material

m_{MNP}: mass of magnetic nanoparticle

5.3. Gas chromatography analysis of gasoline

To see the effect of magnetic heating on specific compounds namely BTEX compounds within Gasoline and Diesel, the heated samples were analyzed using
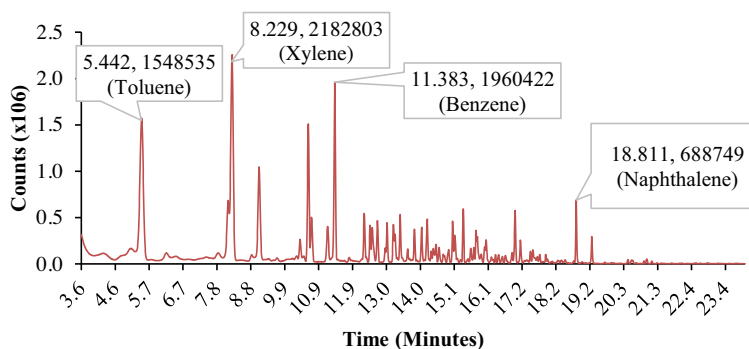

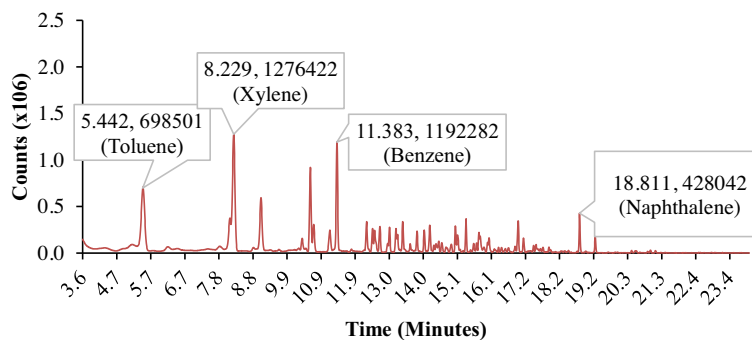**Fig. 8.** Total GC analysis of gasoline before magnetic heating.

Fig. 9. Total GC analysis of gasoline after 75 minutes of magnetic heating.

Gas Chromatography. Fig. 8, and Fig. 9 show the GC analysis of the gasoline-sand-iron mixture before and after magnetic heating for 75 minutes. The x-axes in minutes indicates the time spent inside the GC column. Different compounds take different amounts of time to travel from the injection chamber to the detector. The detector is used to identify the compound type as per GC profiles listed under NIST 14 GC library [23]. The value under count on the y-axes is proportional to the amount of the compound within the hydrocarbon residue with the baseline of 0 count representing the chloroform solvent used in the GC process.

The first few peaks in Fig. 8, and Fig. 9 represent the BTEX compounds within refined gasoline namely Benzene, Toluene, Ethyl-benzene, and Xylene [23]. BTEX compounds are a harmful source of soil and water contamination as per Alberta Tier 1 Guidelines [11]. Desorption/reduction amounts of Gasoline, the
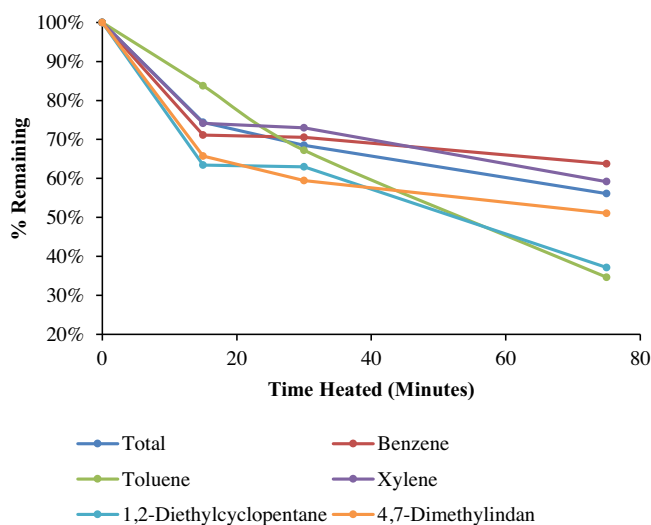

Fig. 10. Percent gasoline and other BTEX compounds after different times of heating. Results measured by peak areas of GC analysis graphs. Note there are multiple peaks that are associated with benzene, other than the one shown in Fig. 8.
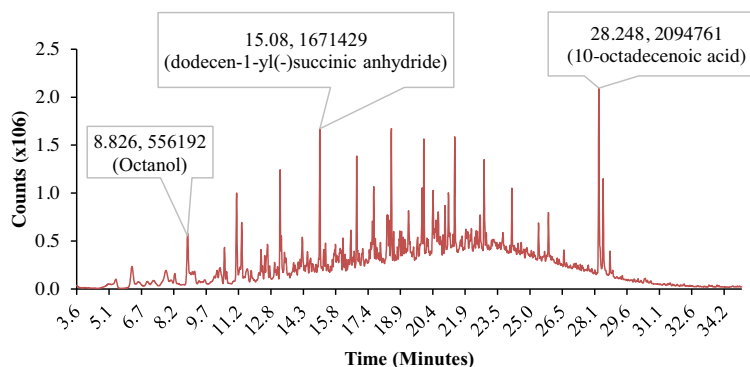
Fig. 11. Total GC analysis of diesel before heating. Note the labeled compounds are a best guess from the NIST database.

individual BTEX, and other prominent compounds within it versus magnetic heating time are plotted in Fig. 10. GC analysis shows that most compounds in Gasoline exhibited similar desorption rates to Gasoline with 56.10% of total gasoline remaining after 75 minutes of magnetic heating.

Of the BTEX compounds in gasoline, Benzene and Xylene were desorbed at the same rate as overall gasoline with 40% of it desorbed after only an hour of magnetic heating. However, Toluene registered a 65% drop/desorption over the same heating period. Toluene (110 °C) has a different boiling point in relation to Benzene (80 °C) and Xylene (144 °C) but is desorbed more quickly by magnetic heating. Exact reasons for this are unknown but can be attributed to the affinity of Toluene to iron as per prior research done on bio-reduction of Toluene in the presence of ferric compounds over a period of days [24].

In addition to BTEX compounds, 1,2-Diethylcyclopentane with a boiling point of 149 °C (a known irritant), exhibited the 2nd highest desorption after Toluene with 63% removal after 75 minutes of magnetic heating [25]. This was followed by 4,7-Dimethylindan with 50% desorbed over the same period [26], [27].
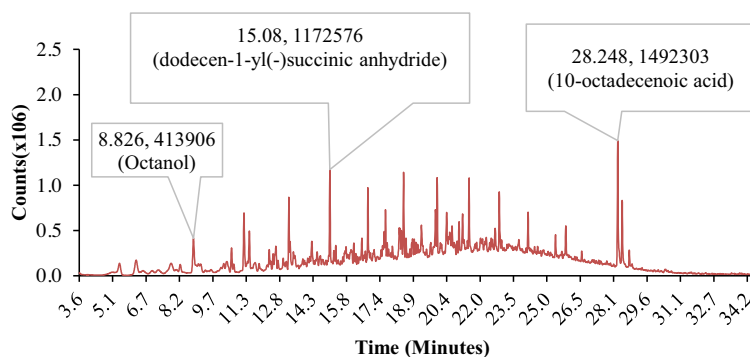

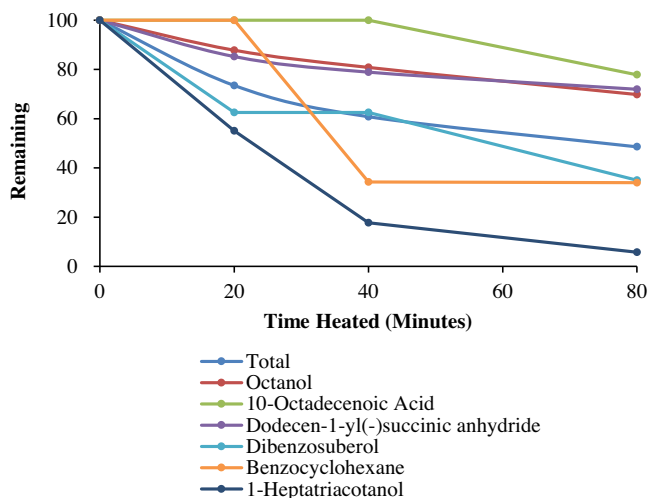**Fig. 12.** Total GC analysis of diesel after 80 minutes of heating.

Fig. 13. Percentage of Diesel after different times of heating.

5.4. Gas chromatography analysis of diesel

Results of Gas Chromatography analysis of the Sand-Diesel-Iron mixture before and after magnetic heating for 80 minutes are shown in Fig. 11 and Fig. 12 respectively. Desorption rates of Diesel overall and specific compounds within Diesel are plotted in Fig. 13. GC analysis shows higher desorption of diesel compared to Gasoline in the fuel-sand-iron mixture with 51.43% of diesel fuel desorbed, compared to 43.9% of Gasoline under the same heating conditions. The higher desorption rate of Diesel is unexpected since Diesel with longer carbon chains tends to be materially heavier than gasoline, which contributes to a higher boiling point.

GC analysis of Diesel shows a higher prevalence of Octanol (Boiling point: 195 °C) and 10-Octadecenoic Acid (Boiling point 369.4 °C, Flash point 266.3 °C), which were desorbed 28% and 22% respectively [28] [29]. Of all the compounds present in diesel, Dibenzosuberol (Boiling point: 166–169 °C), Benzocyclohexane (Flash point: 38–60 °C, Boiling point: 208 °C) and 1-Heptatriacotanol (Boiling

Table 4. Health Side Effects of BTEX Compounds [35, 36, 37].

Compound	% Desorption by magnetic heating	Potential Heath Side effects
Benzene	36	Immune system damage, anemia
Toluene	63	Liver, kidney, central nervous system damage
Xylene	41	Liver, kidney, nervous system damage
1,2-Diethylcyclopentane	63	irritant
Octanol	28	Skin, eye irritant
Benzocyclohexane	66	Skin, eye, and mucous membrane irritant

Table 5. Comparison of magnetic heating results.

Reference	Frequency	Field Strength	Enhancers	Heating Time	Max Temperature (°C)	Mixture
This Paper	117 kHz	3.13 kA/m (Measured)	Iron micrometer size particles	80 min	111	Iron, sand
[13]	10 kHz	44 kA/m	Ferromagnetic nanoparticles	100 s	122	Cobalt-contained iron oxide particles
[39]	266 kHz	75.6 kA/m	Iron Oxide nanoparticles	12 min	47	Iron oxide, phosphate buffer saline solution
[38]	100 kHz	3.5 kA/m	Fe2O3 particles	70 min	95	Commercially available magnetic fluid

point: unknown) registered the most desorption with desorption rates of 65, 66 and 94% respectively [23] [30, 31, 32]. While not as hazardous as BTEX compounds found in gasoline, Octanol and Benzocyclohexane are known irritants to eyes, skin and mucous membranes in animals and humans [28] [31].

5.5. Health effects of hydrocarbon compounds

A summary of harmful compounds found in Gasoline and Diesel and their respective desorption rates with magnetic heating is provided in Table 4. The long term, low concentration health effects of most of the diesel components are insignificant, or they have not been studied in detail [33] [34].

6. Conclusion

The work done in this paper is the first one to study the effects of magnetic heating at over 100 kHz on the desorption of specific compounds within Gasoline and Diesel. Using an easily dispersible, micron-sized iron powder to absorb the magnetic field and generate heat, proved very effective with temperature rises of 130 °C in only 80 minutes.

The use of magnetic fields to remediate hydrocarbons is fairly new, with not many other references to compare this work with. However, magnetic heating has been used in medical heating or ablation applications. A comparison of different magnetic field heating techniques is shown in Table 5. The maximum temperature was found to be dependent on the amount of the enhancer in proportion to the sample size, along with a high imaginary permeability and magnetic field at the heating frequency. Maximizing the magnetic field requires maximizing the NI product of the coil design at the heating frequency as shown in Eq. (2). While [13], [39] and [38] use higher magnetic field intensities, the temperature rise is relatively low compared to this work. This was due to a couple of reasons, one of which being that the coil in this work was designed to have a resonant frequency that lines

up with the frequency where the micrometer sized iron enhancers have higher complex magnetic permeability. Secondly, the use of Litz wire in the coil design for this work makes it possible to achieve a coil impedance that allows for a higher length (N), a higher current output (I) from the current amplifier, and consequently a higher magnetic field intensity at the design frequency as shown in Eq. (2) and Fig. 4.

Although it is hard to compare the fields produced for remediation purposes with fields for medical purposes, it at least shows the variation in frequency, magnetic field strength and heating temperatures acquired.

Gas chromatography analysis on magnetically heated samples show high desorption rates of between 28–66% of Gasoline, Diesel and harmful BTEX compounds and irritants within each hydrocarbon. Due to time, and equipment constraints, longer tests were not done. The heating and desorption trends in Fig. 7, Fig. 10 and Fig. 13 show that the temperature rise of the samples and desorption of hydrocarbons in them would continue to increase with time resulting in better results.

While exact desorption rates of leaking gasoline, diesel and BTEX compounds can vary depending on soil type, conditions, temperature, humidity, depth and area of dispersion of leaked fuels, a rough comparison of a few commonly-used reduction methods of BTEX compounds is shown in Table 6. Methods such as Soil-vapor extraction are carried out by periodically plowing contaminated soil to improve on the evaporation rate of leaked hydrocarbon compounds, but this takes a few months to years for 100% desorption. Anaerobic Degradation and Biopiles involve digs,

Table 6. Comparison of BTEX Extraction Methods.

Method	Compound	Reduction (%)	Time
Magnetic Heating	Benzene	36	75 min
	Toluene	63	
	Xylene	41	
Anaerobic Degradation [24]	Benzene	100	77 days
	Toluene	100	39 days
	Xylene	100	39 days
Anaerobic Degradation [24]	Benzene	36	38 days
	Toluene	63	12 days
	Xylene	41	9 days
Soil Vapor Extraction [40]	All 3	100	Few months − 2 years
Biopiles [40]	All 3	95	6 months − 2 years
Microwave Heating [8], [41]	All 3	99	15 days

aeration, and addition of catalysts to encourage BTEX feeding bio-organisms, which can also take months to years for 100% desorption [5] [7] [24].

Microwave heating has been shown to be very effective as demonstrated in [41]. A comparison of Microwave and Magnetic induction propagation through the ground shows advantages and disadvantages for both techniques. Magnetic fields tend to attenuate faster than Electric (microwave) fields in the far-field away from the radiating coil or antenna. However Electric fields attenuate much more rapidly in clay or wet soil compared to magnetic fields [42].Microwave amplifiers used to transduce the electric fields tend to be class A, which also suffer from a loss of efficiency (50%) compared to current amplifiers. This can be an issue with power usage. The generated 1000–1500 V/m field in microwave heating requires a huge amount of power usage over the 15-day run time, using an unspecified megawatt source Since our solution has not been tested in full-scale, it is unknown how this compares to the power required to generate a 3000 A/m field over a large area with enough penetration to effectively heat the soil.

Magnetic heating can achieve comparable rates of desorption over periods of hours although it will require a more complex and scaled-up design to cover larger volumes. The results of our experiment show that by using low-cost iron filings as an enhancer, hydrocarbons and their harmful compounds can be desorbed by 28–66% from sand in 80 minutes using magnetic heating at 117.8 kHz. This was a small-scale test to determine the effectiveness of this technique. Further research and resources will be needed to show its applications on a full-scale ground remediation.

Declarations

Author contribution statement

Rushi J. Vyas, Bailey S. Tye: Conceived and designed the experiments; Performed the experiments; Analyzed and interpreted the data; Contributed reagents, materials, analysis tools or data; Wrote the paper.

Funding statement

Competing interest statement

The authors declare no conflicting interests.

Additional information

No additional information is available for this paper.

References

[1] Hazmat Magazine, Fill 'er up: The problem of abandoned service station sites, [Online], (2017) . Accessed: 03-Aug-2017 http://hazmatmag.com/2017/01/fill-er-up-the-problem-of-abandoned-service-station-sites/1002520851/.

[2] United States Environmental Protection Agency, Cleaning Up Underground Storage Tank (UST) Releases. [Online], (2017) . Accessed: 03-Aug-2017 https://www.epa.gov/ust/cleaning-underground-storage-tank-ust-releases.

[3] Alberta Energy Regulator, Report -B: Pipeline Performance in Alberta, 1990-2012, (2013) .

[4] T. Lomas-jylha, J. Mullin, How to Unlock Value to Remediate and Redevelop Gasoline Stations, (2017) .

[5] T.T. Tsai, J. Sah, C.M. Kao, Application of iron electrode corrosion enhanced electrokinetic-Fenton oxidation to remediate diesel contaminated soils: A laboratory feasibility study, J. Hydrol. 380 (1-2) (2010) 4–13.

[6] S. Huling, B. Pivetz, Engineering Issue Paper: In-Situ Chemical Oxidation, Engineering (2006) 1–60.

[7] J.J. Pignatello, E. Oliveros, A. MacKay, Advanced Oxidation Processes for Organic Contaminant Destruction Based on the Fenton Reaction and Related Chemistry, Crit. Rev. Environ. Sci. Technol. 36 (1) (2006) 1–84.

[8] P.P. Falciglia, F.G.A. Vagliasindi, Remediation of hydrocarbon-contaminated soils by ex situ microwave treatment: technical, energy and economic considerations, Environ. Technol. 35 (18) (2014) 2280–2288.

[9] F. Vermeulen, B. McGee, In situ electromagnetic heating for hydrocarbon recovery and environmental remediation, J. Can. Pet. Technol. 39 (8) (2000) 24–28.

[10] A. Ligabue, A. Soncini, P. Lazzeretti, The Leap-Frog Effect of Ring Currents in Benzene, J. Am. Chem. Soc. 124 (9) (2002) 2008–2014.

[11] ESRD, Alberta Environment & Sustainable Resource Development, Alberta Tier 1 Soil and Groundwater Remediation Guidelines, (2014) .

[12] H. Hirazawa, H. Aono, T. Naohara, T. Maehara, M. Sato, Y. Watanabe, Heat generation ability in AC magnetic field of nano MgFe2O 4-based ferrite

powder prepared by bead milling, J. Magn. Magn. Mater. 323 (6) (2011) 675–680.

[13] E. Kita, et al., Hysteresis power-loss heating of ferromagnetic nanoparticles designed for magnetic thermoablation, IEEE Trans. Magn. 44 (11) (2008) 4452–4455 PART 2.

[14] D.H. Kim, Y.T. Thai, D.E. Nikles, C.S. Brazel, Heating of aqueous dispersions containing MnFe2O4 nanoparticles by radio-frequency magnetic field induction, IEEE Trans. Magn. 45 (1) (2009) 64–70.

[15] K. Finkenzeller, R. Waddington, RFID Handbook Translated by. (2003).

[16] W.E. Patitz, B.C. Brock, E.G. Powell, Measurement of Dielectric and Magnetic Properties of Soil (1995).

[17] J. Fuzerova, J. Fuzer, P. Kollar, L. Hegedus, R. Bures, M. Faberova, Analysis of the Complex Permeability Versus Frequency of Soft Magnetic Composites Consisting of Iron and Fe73Cu1 Nb3 Si16 B7, IEEE Trans. Magn. 48 (4) (2012) 1545–1548.

[18] Z. Kozakova, I. Kuritka, V. Babayan, N. Kazantseva, M. Pastorek, Magnetic Iron Oxide Nanoparticles for High Frequency Applications, IEEE Trans. Magn. 49 (3) (2013) 995–999.

[19] D.M. Pozar, Microwave Engineering, 2nd edition, Wiley, New York, 1998.

[20] The Engineering Toolbox, Fuels and Boiling Points. [Online], (2017) . Accessed: 03-Aug-2017 http://www.engineeringtoolbox.com/fuels-boiling-point-d_936.html.

[21] International Programme on Chemical Safety, DIESEL FUEL No. 2. [Online], (2017) . Accessed: 03-Aug-2017 http://www.inchem.org/documents/icsc/icsc/eics1561.htm.

[22] R.R. Wildeboer, P. Southern, Q.A. Pankhurst, On the reliable measurement of specific absorption rates and intrinsic loss parameters in magnetic hyperthermia materials, J. Phys. D Appl. Phys. 47 (49) (2014) 495003.

[23] ASD, Atomic Spectra Database | NIST. [Online], (2017) . Accessed: 04-Aug-2017 https://www.nist.gov/pml/atomic-spectra-database.

[24] M.K. Jahn, S.B. Haderlein, R.U. Meckenstock, Anaerobic degradation of benzene, toluene, ethylbenzene, and o-xylene in sediment-free iron-reducing enrichment cultures, Appl. Environ. Microbiol. 71 (6) (2005) 3355–3358.

[25] Royal Society of Chemistry, (1R, 2R)-1, 2-Diethylcyclopentane | C9H18 | ChemSpider. [Online], (2017) . Accessed: 04-Aug-2017 http://www.chem-spider.com/Chemical-Structure.4937993.html.

[26] Royal Society of Chemistry, 1, 2-Dimethylcycloheptane | C9H18 | ChemSpider. [Online], (2017) . Accessed: 04-Aug-2017 http://www.chem-spider.com/Chemical-Structure.122923.html.

[27] Royal Society of Chemistry, 1, 2-Dimethylcyclohexane | C8H16 | ChemSpider. [Online], (2017) . Accessed: 04-Aug-2017 http://www.chem-spider.com/Chemical-Structure.10936.html.

[28] U.S. National Library of Medicine, 1-Octanol | C8H18O – PubChem. [Online], (2017) . Accessed: 04-Aug-2017 https://pubchem.ncbi.nlm.nih.gov/compound/1-octanol#section=Taste.

[29] 10-Octadecenoic acid, C18H34O2 | ChemSpider. [Online], (2017) . Accessed: 04-Aug-2017 http://www.chemspider.com/Chemical-Struc-ture.4445887.html.

[30] U.S. National Library of Medicine, Dibenzosuberol | C15H14O – PubChem. [Online], (2017) . Accessed: 04-Aug-2017 https://pubchem.ncbi.nlm.nih.gov/compound/14588.

[31] 1,2,3,4-Tetrahydronaphthalene, C10H12 – PubChem. [Online], (2017) . Accessed: 04-Aug-2017 https://pubchem.ncbi.nlm.nih.gov/compound/8404.

[32] 1-Heptatriacontanol, C37H76O – PubChem. [Online], (2017) . Accessed: 04-Aug-2017 https://pubchem.ncbi.nlm.nih.gov/compound/537071.

[33] 1-OCTANOL, National Library of Medicine HSDB Database. [Online], (2017) . Accessed: 04-Aug-2017 https://toxnet.nlm.nih.gov/cgi-bin/sis/search/a?dbs+hsdb:@term+@DOCNO+700.

[34] DECANOIC, ACID - National Library of Medicine HSDB Database. [Online], (2017) . Accessed: 04-Aug-2017 https://toxnet.nlm.nih.gov/cgi-bin/sis/search/a?dbs+hsdb:@term+@DOCNO+2751.

[35] R. Kandyala, S.P.C. Raghavendra, S.T. Rajasekharan, Xylene: An overview of its health hazards and preventive measures, J. Oral Maxillofac. Pathol. 14 (1) (2010) 1–5.

[36] Safety and Health Topics, Safety and Health Topics | Toluene - Health Hazards and Protective Measures | Occupational Safety and Health Administration, (2017) . Accessed: 04-Aug-2017 https://www.osha.gov/SLTC/toluene/health_hazards.html.

[37] Centers for Disease Control and Prevention, CDC | Facts About Benzene. [Online], (2017) . Accessed: 04-Aug-2017 https://emergency.cdc.gov/agent/benzene/basics/facts.asp.

[38] M. Bekovic, A. Hamler, Determination of the Heating Effect of Magnetic Fluid in Alternating Magnetic Field, IEEE Trans. Magn. 46 (2) (2010) 552–555.

[39] A.L. Glover, Magnetic Heating of Iron Oxide Nanoparticles and Magnetic Micelles for Cancer Therapy, IEEE Trans. Magn. 49 (1) (2013) 231–235.

[40] F.I. Khan, T. Husain, R. Hejazi, An overview and analysis of site remediation technologies, J. Environ. Manage. 71 (2) (2004) 95–122.

[41] P.P. Falciglia, P. Scandura, F.G.A. Vagliasindi, Modelling of in situ microwave heating of hydrocarbon-polluted soils: Influence of soil properties and operating conditions on electric field variation and temperature profiles, J. Geochemical Explor. 174 (2017) 91–99.

[42] Zhi Sun, I.F. Akyildiz, Magnetic Induction Communications for Wireless Underground Sensor Networks, IEEE Trans. Antennas Propag. 58 (7) (2010) 2426–2435.